On the spherical dust particles in fusion devices

Suk-Ho Hong[1,2], Woong-Chae Kim[1], Yeong-Kook Oh[1], and KSTAR team[1]

[1]*National Fusion Research Institute, 113 Gwahangno, Yusung-Gu, Daejeon, 305-333, Korea*

[2]*Center for Edge Plasma Science (cEps), Hanyang University, Seoul 133-791, Korea.*

Abstract Spherical dusts are present in present tokamaks. Metal droplets and a-C:H nanoparticles of size of 0.1 μm up to 60 μm are observed in many machines including KSTAR. The size distribution and chemical composition of KSTAR metal droplets were analyzed. Due to the material composition, different surface morphology is identified between SUS 316LN and tungsten droplets found in ASEDX Upgrade. Nano- and micro structures on the surface of stainless steel droplets were identified. A large amount of a-C:H nanoparticles is found, and some portions of them are incorporated into thick layers. Tritium retention in a-C:H nanoparticles incorporated into layers will be one of most important problem to be solved in ITER.

1. Introduction

It is now well known that nano- to micron size dusts are present in tokamaks [1, 2]. They are created by several creation mechanisms such as flaking, brittle destruction, arcing, and volume polymerization [3, 4]. Dusts created by flaking and brittle destruction have non-spherical shape while that created by arcing and volume polymerization have spherical shape: Spherical particles are spontaneously formed when critical density of molecules of materials exists in unit volume of plasma, so called "supersaturated vapor condensation". High, localized current during unipolar arcs in tokamaks leads to local erosion of PFCs in a very short time interval which produces metal droplets. Although its creation mechanism and birth place are still under discussion, the presence of hydrogeneted carbon (a-C:H) nanoparticles of size smaller than 1 μm in diameter with a well defined Gaussian size disribution within a certain full-width half maximum (FWHM) is identified in many machines equipped with carbon-based plasma facing components (PFCs). This is a clear evidence of plasma volume polymerization [4] in fusion devices and suggesting that a parameter window for nanoparticle formation exists, even in fusion plasmas.
Existence of the metal droplets and a-C:H nanoparticles in fusion devices arises two interesting questions for future fusion devices like ITER: operational and safety issues. In this paper, we will describe the impact of metal droplets and a-C:H nanoparticles on the operation and safety of the fusion devices.

2. Size Distribution of Spherical Dusts in Fusion Devices

Spherical dusts are created by supersaturated vapor condensation, as we have mentioned before. Other dust creation processes like brittle destruction or flaking of redeposited layers never produces spherical shape. The final size of a spherical dust is depending on the density of the source molecules present in the unit volume. Therefore, the size of metal droplets is connected to both strength and duration of arcs: The stronger/the longer the arc duration is, the more the erosion of a PFC surface is. The more released source material is, the larger the size of a droplet is.

---

[1] sukhhong@nfri.re.kr

* This study is supported by the Korean Ministry of Education, Science and Technology under the KSTAR project.

Metal droplets are frequently found among dusts collected by various methods such as vacuum cleaning [5, 6], sticky adhesive (carbon) tapes [7, 8, 9], specially designed collectors [10, 11], and aerosol catcher [12]. Many fusion devices have reported the presence of metal droplets in the machine observed by Scanning Electron Microscopy (SEM), but the size distributions of them are not systematically analyzed. This is one of the aims of this paper. We report preliminary results obtained from KSTAR.

To have a better statistic along the torus in KSTAR, three different methods were utilized: Dusts were collected by sticky carbon tapes (1st campaign, 10 different toroidal locations) and vacuum cleaner (2nd campaign). 4 pairs of dust collectors were installed at the vertical ports of port D, G, O, and P (2nd campaign, see Fig. 1). The size and chemical composition of collected dusts were analyzed by SEM and Electron Probe X-ray MicroAnalysis (EPMA).

a) b)

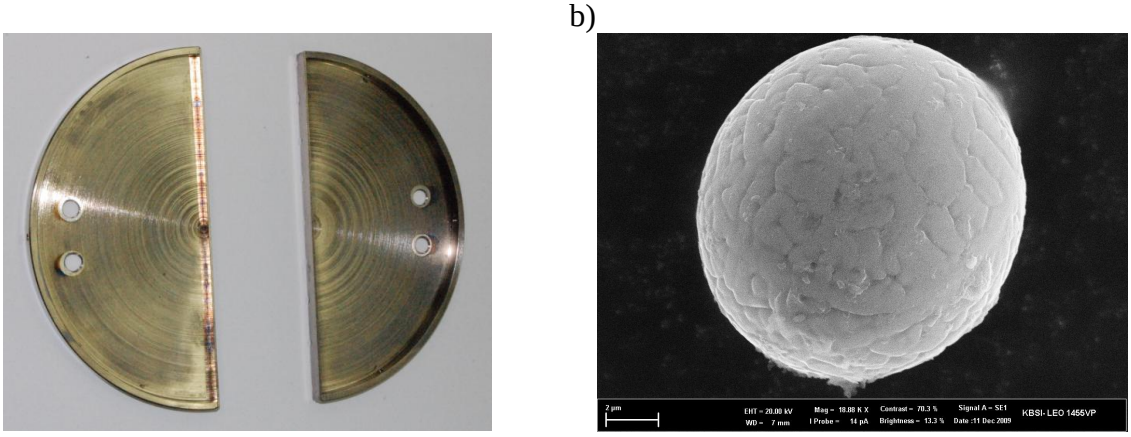

Figure 1. a) KSTAR dust collectors installed at vertical ports in the vacuum vessel. Four pairs of dust collectors were installed. b) A spherical metal droplet of a size of about 13 μm collected in KSTAR.

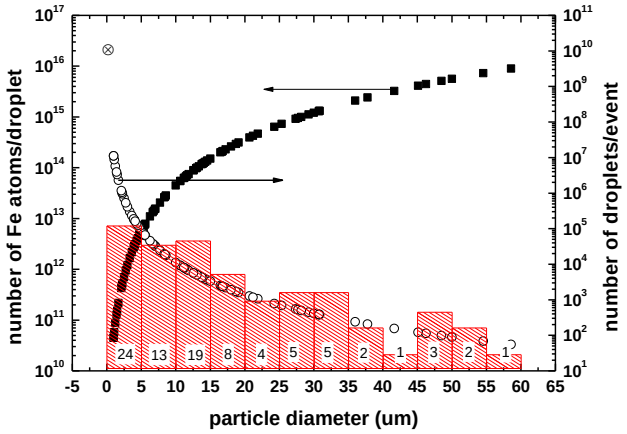

Figure 2. Size distribution of 95 metal droplets collected after the 1st and 2nd campaign in log scale (bars), number of Fe atoms in a metal droplets (closed square), and the total number density of created droplets per arc event (open circles).

Figure 2 shows the size distribution of 95 metal droplets collected after the 1st and 2nd campaign in log scale (bars). The size of the droplets is obtained by 1) directly SEM picture, 2) by conversion from a simple image processing to identify occupied pixel area with the

magnification. Large size droplets of diameters over 1 μm up to 60 μm are identified. As the droplet size increases, the number of droplets decreases rapidly. As we have mentioned above, the size of metal droplets depends strongly on the strength and lifetime of an arc. Arcs induce condensation of eroded materials in a highly localized space in the plasma volume near the PFC where the erosion occurs. From the characteristics of the supersaturated vapor condensation in dusty plasmas [13], larger droplets would be created by stronger arcs: A strong arc erodes the PFC material quicker and deeper. Therefore, the condensation occurs much quickly due to the abundance of source material in unit volume. Moreover, a stronger arc provides much higher temperature during the condensation. As a result, droplets can grow up much faster to a larger size. On the other hand, weak or quickly moving arcs provide relatively less source material into the unit volume, thus much smaller but a large amount of droplets would be produced. The measured metal droplet size distribution in Fig. 2 suggests that smaller arcs were dominant in KSTAR. Furthermore, droplets were found everywhere regardless toroidal position in the vacuum vessel.

Typical arc duration is less than 1 ms, and typical arc tracks from limiters and divertors have dimensions of 10 μm in depth, 10-100 μm in width, and 5-10 mm in length [3]. This gives 10^{17}-10^{18} atoms of eroded material per arc event [3]. Applying the numbers to the measured size distribution in Figure 2, total Fe atom in a droplet (closed square, see also below) and the number of droplet produced by arc event (open circle) are obtained. A material density of 8 g/cm^3 (Fe) is assumed. The symbol ⊗ in Figure 2 is calculated value for 0.1 μm droplet as a lower limit: A 0.1 μm droplet has ~4.48×10^{9} Fe atoms/droplet (4.19×10^{-13} g), while ~60 μm droplet has ~9.0×10^{15} Fe atoms (8.42×10^{-7} g). Using 5×10^{17} as an average number of eroded Fe atoms per arc event [3], 1.12×10^{10} droplets with a diameter of 0.1 μm is obtained, while 55.56 droplets is calculated for a diameter of 60 μm.

Amorphous hydrogenated carbon (a-C:H) nanoparticles are found in many tokamaks. Figure 3 shows a-C:H nanoparticles collected at JET [14] and b) at KSTAR. The size of a-C:H nanoparticles found in fusion devices were much smaller, about 100 nm in diameter. Average size of a-C:H nanoparticles at JET is ~0.1 μm, and that in KSTAR is ~0.1-1 μm. Nanoparticles found in Tore Supra has a smaller size of ~0.02-0.07 μm [15], less than ~1 μm in LHD [16]. Note that, the birth place of a-C:H nanoparticles in fusion device is still in controversy, but their existence in fusion devices strongly suggests that there is an parameter window in which plasma volume polymerization takes places. Furthermore, they are quite homogeneously distributed in torus: GDC can be ruled out, since the nanoparticle size found in fusion devices is too small to be created and grown up during several hours of GDCs. GDC can provide a large amount of hydrocarbon species and a strong sheath in which nanoparticles can be trapped and grown up to several μm before the force balance between electric force and gravitational force is broken (depending on charge to mass ratio e/m). Size less than 1 μm also indicates that the growth time of the particles in the plasma was short: In a low temperature RF methane plasma, the average growth speed of a-C:H nanoparticles was several ten nanometer per sec [17]. A larger amount of source material leads to a faster growth speed [17]. Arcs on the surface of a carbon PFC can produce a-C:H nanoparticles. Indeed, a large amount of arc tracks were found on the surface of poloidal limiter, e.g., attached to the ICRH antenna at port O in KSTAR. If this is the major creation process of the a-C:H nanoparticles, they have to be survived and transported through the plasma without destruction, in order to explain homogeneous distribution in torus and non-destroyed surface sutrcture. Figure 4 shows a-C:H nanoparticles after plasma-dust interaction in laboratory and metal droplets in KSTAR. It is clearly seen from the pictures than the surface structures were heavily modified. This reveals that arcs are not the main creation mechanism of a-C:H

nanoparticles. Another possibility is detached plasma or Multifaceted asymmetric radiation from the edge (MARFE), because the density and temperature are in the similar range with that in low temperature dusty plasmas [18].

a) b)

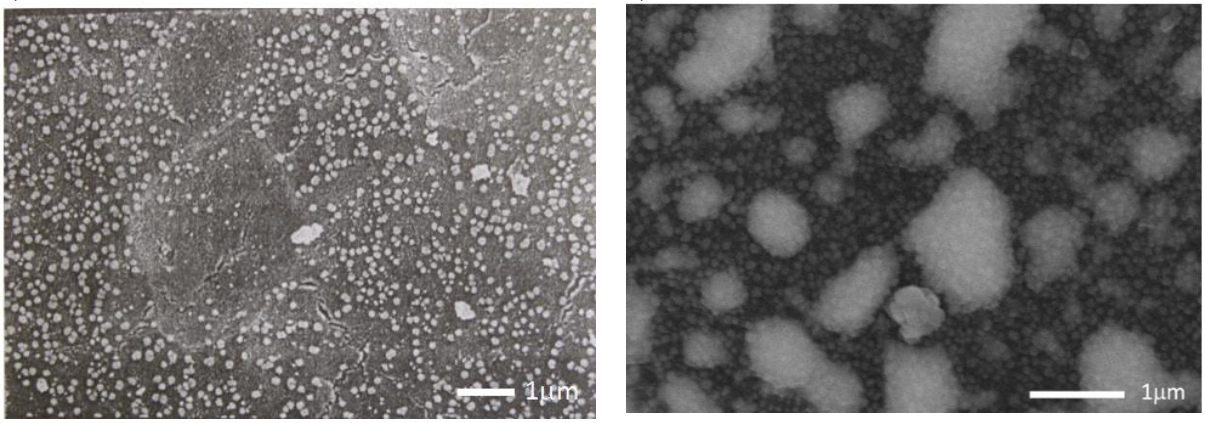

Figure 3. a) a-C:H nanoparticles collected at JET [14] and b) at KSTAR. A large amount of nanoparticles are agglomerated.

a) b)

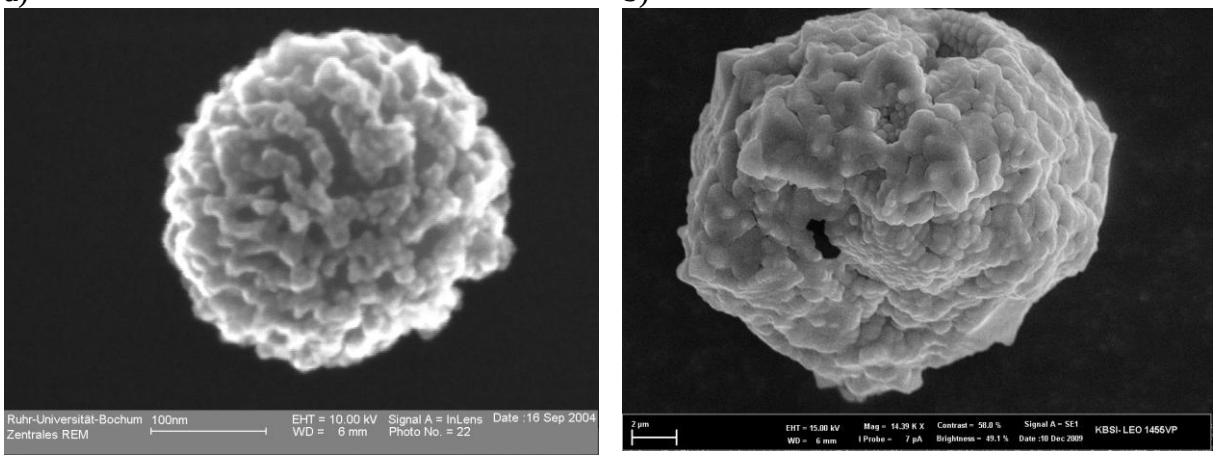

Figure 4. Spherical dusts after plasma-dust interaction. a) a-C:H nanoparticles in laboratory b) metal droplet in KSTAR. At the top, three successive micro-crystal layers (see Fig. 5a also) ensure that it was originally a metal droplet as shown in Fig. 4a) and 5a).

3. Chemical Composition of Spherical Dusts

Chemical composition of KSTAR metal droplets was measured by EPMA. The beam size of a conventional EPMA is 1-3 μm in diameter, thus the chemical composition of large size metal droplets can be easily measured. The composition of smaller a-C:H nanoparticles can be measures only when they are agglomerated into a larger ones as shown in Figure 3 b). Figure 4 shows metal droplet under EPMA measurement and the EPMA peaks using LIF crystal. Table 1 and 2 show the weight/mol % of main chemical elements found in stainless steel metal droplets. As expected, the main chemical compositions of droplets are Fe, Cr, Al, and O that are the main components of stainless steel 316LN (materials for vacuum vessel) - Fe, Cr, and some % of Al - and metal oxides. 27 % of molecular weight is oxygen, which

exists in the form of metal oxides (table 2). This indicates that a large amount of oxygen was present in the vacuum vessel (see Ref [19]).
For a-C:H nanoparticles, we have obtained only carbon signals, because hydrogen is not detectable by EPMA.

a) b)

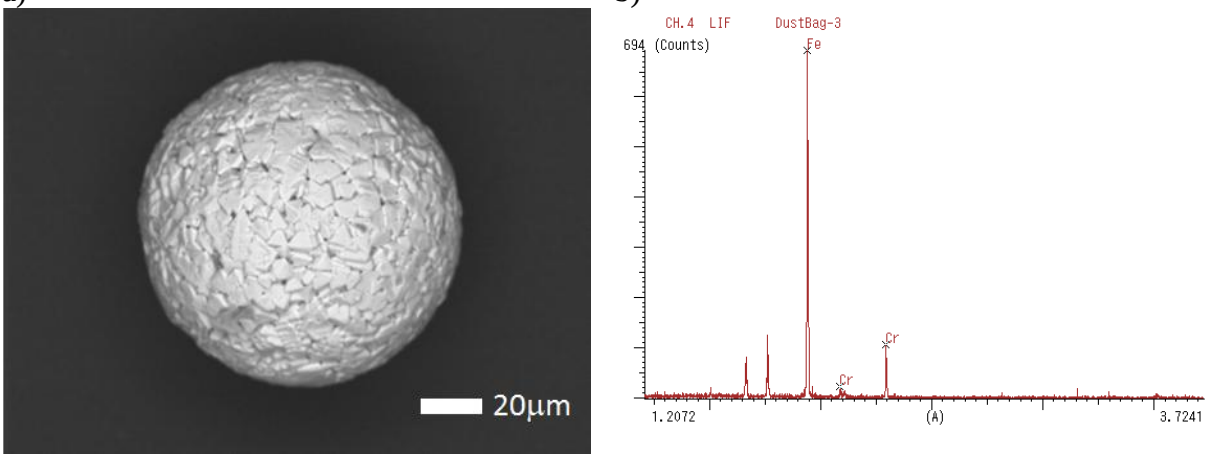

Figure 4. a) metal droplet under EPMA measurement b) EPMA peaks using LIF crystal. Main chemical compositions are Fe and Cr.

Element.	Weight (%)	Mol(%)
Fe	61.801	36.734
O	27.059	56.142
Cr	9.419	6.013
Br	1.236	0.513
Al	0.0086	0.597

Table 1. chemical elements of metal droplets, their weight % and Mol %.

Oxide	WT(%)	Mol(%)
FeO	84.132	90.819
Cr_2O_3	12.018	6.132
BrO	2.502	2.023
Al_2O_3	1.348	1.026

Table 2. weight % and Mol % of metal oxide in droplet.

4. Surface morphology and Internal Structure of Spherical Dusts

Surface morphology of spherical dusts produced by volume polymerization has a specific characteristic. Nanoparticles have a surface structure, so called “cauliflower-like” structure. This structure is due to the accretion of ions and neutrals on the surface of the nanoparticles. Actually, nanoparticles larger than about 100 nm in diameter react as a flat surface to incoming species. Thus, the growth of the nanoparticles through accretion is almost the same as thin film deposition on a flat sample [20]. Evolution of surface roughness and fractal nature cause such surface morphology. The internal structure of a-C:H nanoparticles were identified by and micro-Raman spectroscopy [20], in-situ Rayleigh-Mie ellipsometry [21] by Hong et al. Nanoparticles have internal shell structure with different H/C ratio [20] (see below).
Metal droplets, however, show two different surface structures depending on the composition: tungsten droplets have flat surface structure like a billiard ball [22], while

stainless steel droplets have nano- or micro crystal structure on the surface (see Fig. 1 and 4). The difference would come from the crystallization of the material. As an arc strikes the material and after the metal droplet formation, the temperature of the droplets is high, even they can be detected by visible CCD cameras due to radiation in visible range. High heat flux is applied to a highly localized point, thus the temperature of droplets can be as high as melting point of the material. Tungsten has highest melting point of over 3400 ℃ while SUS 316LN has lower about 1300 ℃. Recrystallization temperature of tungsten is about 1300-1500 ℃, and that of SUS 316LN is 700-900 ℃. If other chemical components are present, the recrystallization temperature can be varied: Figure 4 and 5 a) show clearly the recrystallization of SUS 316LN droplets. Furthermore, it seems that the recrystallization takes place also inside the droplets that they have also onion-like internal structure (Figure 5a), which is broken into smaller pieces of size of about 2 μm. This would be important for ITER first wall, because beryllium has similar melting temperature of 1287 ℃ as SUS 316LN, the recystallization temperature is slightly lower (1254 ℃). ITER-like Be PFC experiment in JET shows melting of the Be tile edge during high power/low density operation and formation of Be droplets [23]. Divertor temperature was reached ~1300 ℃ [23]. It is expected that Be recrystallization would occur, but still no analisys of collected Be droplets from JET.

a) b)

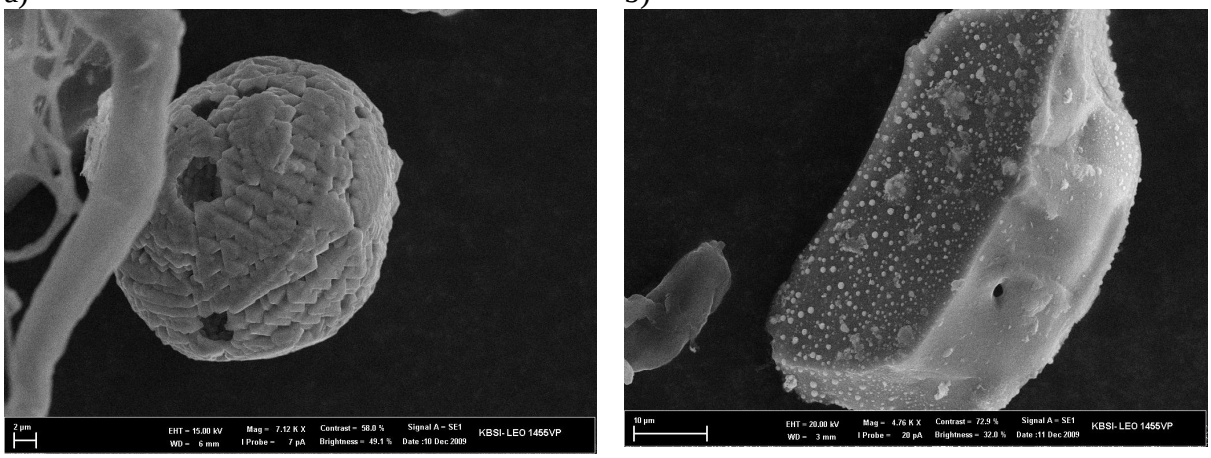

Figure 5. a) metal droplet with nano-crystal surface and onion-like shell structure b) thick redeposited layer with incorporated a-C:H nanoparticles

5. Impact on ITER operation and Safety

From the previous section, it is obvious that large size metal droplets do not always remain as they are created, but some parts of micro-structures are broken into smaller pieces. This could be one of serious problems in future devices like ITER. According to ITER accidental scenario, metal dusts can react with air if vacuum is broken. Micro-size metal dusts will react with oxygen, leading to an explosion due to the oxidation.

Another striking fact observed in KSTAR is the incorporation of a-C:H nanoparticles into layers at vertical ports (Figure 5b). Layers deposited by hydrocarbon-based chemical reactions have two different characteristics. If the energy of impinging ions is low, the layers have low density with soft polymer-like characteristics. If the energy of impinging ions is high, the layers have high density with hard diamond-like characteristics. Hard a-C:H films have very strong internal stresses so that they pile off from the surface of the substrate where they are deposited when their thickness exceeds the limit (usually 0.5-1 μm) [4]. From the

technical point of view, the limitation of the deposition thickness of a hard a-C:H thin film can be overcome by hydrogen removal [24], or by incorporation of small nanoparticles into the layer [4].
Figure 5b) clearly reveals two very important facts for ITER operation and safety. First of all, these small nanoparticles would have no effect on the operation, especially for start up, because they are tightly bonded to the layers. Recent DIII-D observation during the ITPA urgent task "injection of pre-calibrated dust" indicates that dusts can be mobilzed before the plasma start up and they disturb the start up. On the other hand, although ITER uses full tungsten divertor during D-T phase, carbon will be present in the machine due to the co-deposited layers at shadow regions. There is always possibility that a-C:H nanoparticles are formed during ITER operation: It is found that a-C:H nanoparticles have onion-like internal shell structures [20, 21]. Inner shell ($r<50$ nm) has small amount of hydrogen ($H/C\sim0.4$) due to high temperature during the growth of nanoparticles, but outer shell ($r>50$ nm) has H/C ratio larger than 1. As soon as ITER uses tritium, the T retention in the a-C:H nanoparticles created in the D-T phase can be significant. Recent calculation of T retention in hydrocarbon nanoparticles in ITER during a MARFE in D-T phase with 1% of carbon impurity density by Hong et al is about 3.6 g [18]. As we have mentioned above, detached plasma has similar characteristics. Partially detached operation in ITER would create a-C:H nanoparticles. Once these nanoparticles are incorporated into layers, layers can grow easily up to several ten to hundred μm due to stress relaxation by nanoparticles, and tritium incorporated into nanoparticles cannot be collected unless entire layers are removed.

6. Conclusion and Outlook

Spherical dusts are present in tokamaks. They will be potential threat for ITER safety and operation. Creation of metal droplets by arcs and smaller pieces generated by recrystallization of the materials make a large population of micro-meter size dusts that have much larger specific surface area. In the case of air ingress, they will react with oxygen. Tritium retention in a-C:H nanoparticles incorporated into layers will be one of most important problem to be solved. ITER operation will not be affected by ELM, structural failure, broken component, but tritium retention limit of 700 g. If the limit is reached, ITER has to stop the operation and remove tritium from the vacuum vessel. Otherwise, ITER cannot operate further: The impact of a-C:H nanoparticles on ITER would be significant than we have expected: ITER *should not use carbon divertor* at all from the beginning of D-D phase.

Acknowledgements

* This study is supported by the Korean Ministry of Education, Science and Technology under the KSTAR project.

References

[1] J. Winter , Dust: a new challenge in nuclear fusion research. *Phys. Plasmas* 7 (2000), 3862
[2] J. P. Sharpe el al, Fusion Engineering and Design, 63-64 (2002), 153
[3] G. Federici, et al., Plasma–material interactions in current tokamaks and their implications for next-step fusion reactors, External Report PPPL-3512, IPP-9/128, January, 2001.
[4] S. Hong, 2004, *PhD Thesis*, Ruhr-University Bochum, Bochum, Germany
[5] J. Winter, Plasma Phys. Control. Fusion 40 (1998) 1201
[6] C. Grisolia *et al.*, *J. Nucl. Mater.* 390–391 (2009), 53.

[7] S. H. Hong et al., EPS 36, 29 June - 3 July, 2009, Sofia (Bulgaria), http://epsppd.epfl.ch/Sofia/pdf/P1_099.pdf
[8] S. Muto et al., *J. Nucl. Mater.* 307–311 (2002), p. 1289
[9] S. Rosanvallon et al., *J. Nucl. Mater.* 390–391 (2009), p. 57
[10] S. H. Hong, IAEA CRP(2008-2012): Characterization of Size, Composition and Origins of Dust in Fusion Devices, http://www-amdis.iaea.org/w/index.php/In-vessel_dust_research_in_KSTAR:_preliminary_results_on_flakes,_metal_droplets,_and_nanoparticles
[11] V. Rohde et al., Phys. Scr. T138 (2009) 014024
[12] C. Castaldo, IAEA CRP(2008-2012): Characterization of Size, Composition and Origins of Dust in Fusion Devices, http://www-amdis.iaea.org/w/index.php/Detection_of_fast_dust_particles_in_tokamaks_by_aerogel_samples_and_electro-optical_probes
[13] A. Bouchoule, Dusty Plasmas: Physics, Chemistry, and Technological Impact in Plasma Processing, John Willey & Sons LTD, ISBN 0-471-97386-6, (1999)
[14] A. C. Francis and J. Foster, "Analytical results and data for JET in-vessel flakes after DTE1", Technical report, JET, 1999
[15] P. Roubin et al., J. Nucl. Mater. 390–391 (2009) 49
[16] N. Ashikawa, IAEA CRP(2008-2012): Characterization of Size, Composition and Origins of Dust in Fusion Devices, http://www-amdis.iaea.org/w/index.php/Update_on_characterization_of_dust_and_its_dynamics_in_LHD_and_JT-60U
[17] S. H. Hong et al., Plasma Sources Sci. Tech. 12, (2003) 46
[18] S. H. Hong et al., EPS 34, 1-10 July, 2007, Warsaw (Poland), http://www.iop.org/Jet/fulltext/EFDP09024.pdf
[19] S. H. Hong et al., "initial wall conditioning in KSTAR" in this proceedings
[20] S. H. Hong and J. Winter, J. Appl. Phys. 98, (2005) 124304
[21] S. H. Hong and J. Winter, J. Appl. Phys. 100, (2006) 064303
[22] V. Rohde et al., A. Herrmann et al., J. Nucl. Mater., 390-391 (2009) 747
[23] A. Loarte, J. Nucl. Mater. 337-339 (2005) 816
[24] Jang, J., Chung, S. J., International Journal of Modern Physics B, Vol. 14, Nos. 2 & 3, 154-166 (2000)